Available online freely at www.isisn.org

Bioscience Research

Print ISSN: 1811-9506 Online ISSN: 2218-3973

Journal by Innovative Scientific Information & Services Network

RESEARCH ARTICLE BIOSCIENCE RESEARCH, 2024 21(1):132-142. **OPEN ACCESS**

Induction of autophagy by genotype F mumps virus in Vero cells

Hongna Wang

Affiliated Cancer Hospital and Institute & Guangzhou Medical University, No. 78 Hengzhigang Road, Yuexiu District, Guangzhou, 510095, Guangdong, **People's Republic of China**

***Correspondence:** wanghn110@126.com **Received: January 01, 2024, Revised: February 06, 2024, Accepted: February 08, 2024 e-Published: February 12, 2024**

Despite the widespread administration of the Mumps virus (MuV) vaccine, which has significantly reduced the incidence of epidemic parotitis, sporadic outbreaks persist worldwide, occasionally affecting vaccinated populations. Consequently, there is an urgent need to comprehend the intricate molecular biology of MuV, particularly its interplay with host factors. Autophagy, a pivotal immune mechanism within host cells, is critical in protecting against viral infections by selectively sequestering and degrading viral components via autophagosomes. Nonetheless, our current understanding of the reciprocal relationship between MuV and autophagy remains limited. This study substantiates this interaction through transmission electron microscopy, confocal microscopy, and Western blot analysis. We directly ascertained the appearance and accumulation of pre-autophagosomal structures, autophagosomes, and autolysosomes within Vero cells following genotype F MuV infection. Evidential markers include the redistribution and lipidation of the autophagic indicator LC3 within infected cells, an increase in punctate lipidated LC3, and the presence of cup-shaped phagocytic vesicles, double-membrane autophagosomes, as well as notably large (2-8 µm) single-membrane structures, as observed through electron microscopy. Immunostaining further demonstrated that this prominent structure exhibited positive signals for both LAMP1 and MuV capsid, thereby establishing its identity as an autolysosome encapsulating MuV components. Additional ultrastructural observation of the virus budding process showed consistent results. Our findings demonstrate that MuV could stimulate autophagy in the continuous cell line Vero, thus providing insight into the host-virus interaction.

Keywords: genotype F; mumps virus; MuV; autophagy; LC3; replication; Vero

INTRODUCTION

Mumps, an abbreviation for epidemic parotitis, is an acute respiratory infectious disease caused by the mumps virus (MuV). It is distinguished by the swelling of the parotid glands, occurring either unilaterally or bilaterally (Briggs et al. 2020; Zhang et al. 2023). Following a 2-4 week incubation period, the infection manifests as mild fever, headache, and malaise, which are commonly followed by parotid gland swelling. MuV spreads systemically throughout the body after initially infecting the upper respiratory mucosa and local lymph nodes. And mumps is recognized for its potential to give rise to various complications, including conditions like encephalitis, orchitis, oophoritis, myocarditis, and arthritis (Shan et al. 2021; Gokhale et al. 2023). The widespread implementation of mumps vaccination has substantially diminished the occurrence of mumps. Nevertheless, sporadic mumps outbreaks continue to arise globally, and mumps can resurge within populations even post-vaccination (Rubin et al. 2012; Connell et al. 2020). Notably, MuV does not only lead to parotitis but also triggers systemic infections. However, the mechanism through which MuV penetrates the epidermal barrier to facilitate systemic infection remains unclear. Moreover, MuV has been used as an oncolytic virus to treat cancer patients in Japan in the 1970s and 1980s (Ammayappan et al. 2016). Yet the molecular and cellular mechanisms of cancer cell destruction by MuV are not fully elucidated. Thus, it is imperative to comprehend the intricate molecular biology of MuV, especially about its interactions with host factors.

MuV is a member of the *Rubulavirus* genus within the *Paramyxoviridae* family. It possesses a single-stranded negative-sense RNA genome, spanning a length of 15,384 base pairs. The MuV genome is organized in a 3'-5' orientation and encodes a distinct sequence of proteins: nucleocapsid protein N, phosphoprotein P, matrix protein M, fusion protein F, small hydrophobic protein SH, hemagglutinin-neuraminidase HN, and large protein L (Forgione et al. 2020). Analogous to the replication and translation mechanisms observed in other single-stranded negative-sense RNA viruses, MuV's HN

protein binds to cell surface receptors, notably sialic acid. This interaction triggers a conformational alteration in the F protein, ultimately facilitating fusion between the viral envelope and the host cell membrane. Following this fusion, the virus enters the cell, extricates its envelope, and liberates its genomic material (Kubota et al. 2016, 2019). Guided by the virus's intrinsic P protein and the RNA-dependent RNA polymerase L, the negative-sense RNA genome is employed as a template. Initially, it transcribes messenger RNA (mRNA) encoding structural proteins, followed by their translation. Simultaneously, the positive-sense genome (antigenome) is transcribed from the negative-sense genome. By utilizing the antigenome as a framework, progeny viral genomes are transcribed. Upon combining with translated viral proteins, these genomes assemble into fresh progeny viruses via the budding process (Zhang et al. 2023). The *SH* gene has the highest number of sequence variations, making it commonly used for the standardized nomenclature of MuV. Based on the SH and HN sequences of the MuV genome, the World Health Organization (WHO) assigned standard names for the 12 MuV genotypes by the letters A to N (excluding E and M) in 2012 (Su et al. 2020).

In the context of the sparse investigations into MuV replication and its interactions with the host, Katoh et al. have indicated that the intracellular transport of MuV ribonucleo protein complexes (RNPs) in polarized cells, notably Vero and MDCK cells, relies on the Rab11-positive endosomal pathway. Rab11 is a member of small GTPases that regulate vesicular transport in endosome/lysosome recycling (Guichard et al. 2014). The impairment of Rab11 function leads to a marked reduction in viral release from these polarized cells (Katoh et al. 2015). Complementary findings from Ueo *et al.* propose direct interactions between lysosomal-associated membrane proteins (LAMP1, LAMP2, and LAMP3) and the MuV F protein, facilitating furin-mediated processing of the viral F protein (Ueo et al. 2020). These insights collectively suggest a potential correlation between the endocytic and lysosomal vesicular system and MuV replication dynamics. Through the intentional overexpression of the F protein, Sébastien Delpeut et al. provocatively induced autophagy within Vero cells (Delpeut et al. 2012). In a related context, Han *et al.* observed MuV's capability to infect supportive and stromal cells in mouse testicular tissue, while sparing spermatogenic cells due to their comparatively elevated autophagic activity. The perturbation of autophagy through the administration of the autophagy inhibitor 3-methyladenine (3-MA) resulted in a notable augmentation of MuV presence within spermatogenic cells, implying a safeguarding role of autophagy against MuV intrusion (Wu et al. 2017). These parallel inquiries collectively underscore a potential nexus between autophagy and MuV. Autophagy represents a highly conserved cellular degradation process through lysosomes. However, the specific involvement of autophagy in the regulatory dynamics of MuV remains an area of limited understanding.

This research delved into the presence of autophagy-associated indicators within Vero cells upon genotype F MuV infection. This encompassed the examination of markers such as LC3, indicative of autophagy, and the characterization of autophagic ultrastructures. By employing transmission electron microscopy, we directly ascertained the appearance and accrual of pre-autophagosomal structures, autophagosomes, and autolysosomes within Vero cells following MuV infection. These outcomes collectively suggest a concomitant activation of the autophagic process alongside the replicative stages of MuV within the Vero cell lineage.

MATERIALS AND METHODS

Cells and viruses:

Vero E6 cells were grown in Dulbecco's modified Eagle's medium (DMEM) containing supplements (10% fetal bovine serum, 2 mM glutamine, 100 U/mL penicillin, 100 mg/mL streptomycin). Cells were cultured at 37°C in a CO_2 atmosphere with 95% humidity. The genotype F MuV strain SP-A was kindly provided by Dr. Daishu Han (School of Basic Medicine, Peking Union Medical College). A virus stock was generated by infecting Vero E6 cells at low infection multiplicity (0.01 PFU/cell). When the cytopathic effect (CPE) was evident (4-7 days post-infection), the supernatants were clarified by low-speed centrifugation and stored in aliquots at -80°C until use. MuV was amplified and titrated in Vero cells. MuV preparations were stored at -80°C. For infection, cells were grown to approximately 80% confluence and then inoculated with MuV for 2 h or mock-infected with the same volume of medium. After 2 h absorption at 37°C, the inoculum was removed, and the cells were washed twice with PBS and further incubated in maintenance media (DMEM containing 2% FBS) at 37°C for different times until harvesting of the cells.

Antibodies

Rabbit anti-LC3B polyclonal antibody (NB100-2220) was purchased from Novus Biologicals (Colorado, USA). Rabbit monoclonal antibody against β-actin (AC026) was purchased from ABclonal Biotech (Wuhan, China). Mouse monoclonal antibodies against MuV N protein for immunofluorescence (ab9876) and immunoblot (ab9880) were purchased from Abcam (Cambridge, UK). Rabbit monoclonal antibody against LAMP1 (D2D11) (9091) was purchased from Cell Signaling Technology. Horseradish peroxidase (HRP)-conjugated secondary antibodies were purchased from purchased from Cell Signaling Technology (Danvers, MA, USA). Alexa Fluor 488-conjugated goat anti-rabbit and Alexa Fluor 568-conjugated goat anti-mouse secondary antibodies

for western blotting were purchased from Invitrogen (California, USA).

Plaque assay

MuV titers were assessed using plaque assay in Vero cells. Briefly, Vero cells were cultured in 6-well plates at 2 × 10^5 cells/well and infected with a serial dilution of MuV for 1 h. After removing the inoculate, cells were washed three times with PBS and then cultured in MEM containing 1% FCS and 1.2% Avicel RC581 (Pythonbio). After further incubation for 4-7 days, overlays were removed, and cells were stained with 1% crystal violet solution (Sigma-Aldrich) in accordance with the manufacturer's instructions. Plaques were counted according to the following formula:

Pfu/mL=Average number of plaques/D*V,

D=dilution, V=volume of diluted virus added to the plate

Immunofluorescence staining

Cells grown on polylysine-coated coverslips were fixed in 4% paraformaldehyde (PFA) for 10 min and washed 3 times in PBS. Then, after blocking/permeabilization with 0.2% saponin in 5% bovine serum albumin (BSA) for 30 min, slides were incubated with primary antibody (1:500, polyclonal anti-LC3B, Novus Biologicals; 1:10, monoclonal anti-MuV-N, Abcam; 1:800, monoclonal anti-LAMP1, Cell Signaling Technology) diluted in 1% BSA at 4°C overnight. After washing with PBS, the sample was incubated with Alexa Fluor 488- or Alexa Fluor 568-conjugated secondary antibody diluted in PBS for 1 h at 37°C. Next, the slides were washed in PBS, and nuclei were stained with 4',6-diamidino-2-phenylindole (DAPI). Images were collected with the 60× oil-immersion objective lens of a confocal laser scanning microscope (LSM 880; Zeiss, Germany) and acquired by using ZEN software (Zeiss). 405-nm violet laser, 488-nm blue laser, and 561-nm green laser were used. Single focal plane images were captured and are represented in figures.

Western Blot

Adherent cells were scraped off the dish using a cold plastic cell scraper, and then gently transferred into a pre-cooled microcentrifuge tube. Cells extracts were prepared using a Dounce homogenizer in cold lysis buffer (25 mM Tris-HCl, pH 7.6, 150 mM NaCl, 1% Nonidet P-40, 1% sodium deoxycholate, 0.1% sodium dodecyl sulfate) supplemented with 1 mM phenylmethylsulphonyl fluoride and protease inhibitor cocktail (Roche). The homogenates were centrifuged at 12,000 rpm for 15 min, and protein concentrations were determined using the Pierce BCA Protein Assay Kit. Protein extracts were denatured in Laemmli sample buffer (2% SDS, 6% glycerol, 150 mM beta-mercaptoethanol, 0.02% bromophenol blue, and 62.5 mM Tris-HCl pH=6.8). Equal amounts of lysates (25 µg) were separated in 4 to 12% Bis-Tris gel and separated by sodium dodecyl sulfate-polyacrylamide gel electrophoresis (SDS-PAGE). Then, the gel was transferred to a hydrophilic polyvinylidene fluoride (PVDF) membrane using Trans-Blot® Turbo™ Blotting System (BioRad) following the manufacturer's protocol. The membranes were blocked in 5% Difco™ Skim Milk (BD Life Sciences) in PBS with 0.1% Tween 20 (PBS-T) and probed with primary antibody overnight at 4°C. Following 3 washes with PBS-T, the membranes were incubated with a secondary antibody for 1h at room temperature, washed 3 more times in PBS, and incubated with Super Signal West Pico (Thermo Fisher Scientific), and protein luminescence was detected by a Tanon 5200 Image Analyzer (Shanghai, China).

Transmission electron microscopy

Cells were fixed with a solution containing 2.5% glutaraldehyde and 2% paraformaldehyde in 0.1 M cacodylate buffer (pH 7.2). Samples were then washed in 0.1M sodium cacodylate buffer and treated with 0.1% Millipore-filtered cacodylate buffered tannic acid, post-fixed with 1% buffered osmium and stained en bloc with 0.1% Millipore-filtered uranyl acetate. The samples were dehydrated in increasing concentrations of ethanol and then infiltrated and embedded in the LX-112 medium. The samples were then polymerized in a 60°C oven for approximately three days. Ultrathin sections were cut using a Leica Ultracut microtome (Leica, Deerfield, IL) and then stained with uranyl acetate and lead citrate in a Leica EM Stainer. The stained samples were examined in a JEM 1400 transmission electron microscope (JEOL USA, Inc., Peabody, MA) using an accelerating voltage of 80 kV. Digital images were obtained using an AMT imaging system (Advanced Microscopy Techniques Corp., Danvers, MA).

Quantification and statistical analysis

The band intensity for the western blot was quantified using densitometry with Image J software (https://fiji.sc). To measure only the LC3 puncta, we eliminated background signals for the same value in all images when using Zen software. Consequently, spots that have values greater than a certain fluorescence intensity were quantified. All data are presented as mean ± SEM. The statistical significance of the difference between the mean values for the different genotypes was measured by Student's t-test with paired, 2-tailed distribution. The data were considered significant when the P value was less than 0.05 (*) or 0.01(**).

RESULTS

MuV infection induces LC3 redistribution and lipidation

Microtubule-associated protein 1A/1B-light chain 3 (LC3) is a ubiquitously present soluble protein in mammalian tissues. Two forms of LC3 have been reported. LC3-I, the precursor form of LC3, resides in the

cytoplasm in a diffused pattern in quiescent cells. However, upon exposure to various autophagy stimuli, it is rapidly modified and conjugated to phosphatidylethanolamine (PE) to form a lipidated form LC3-PE. LC3-PE is commonly referred to as LC3-II, which shows a dotted-like distribution and is localized to isolation membranes and autophagosomes (on both inner and outer membranes). Therefore, LC3 is currently the most widely used autophagosome marker because the amount of LC3-II reflects the number of autophagosomes and autophagy-related structures (Noboru Mizushima and Beth Levine, 2010; Yoshii and Mizushima, 2017). To determine whether MuV infection triggers cellular autophagy in Vero cells, we investigated the distribution of LC3 by immunofluorescence upon virus infection. Cell monolayers were inoculated with genotype F MuV SP-A strain at an MOI of 0.1 (Figure 1A, red dots). In uninfected cells, LC3 was dispersed throughout the cytoplasm. Post-infection, conspicuous LC3 II puncta accumulated (Figure 1A, white arrows), indicating LC3 type I conversion to type II and autophagy activation (Figure 1B). Studies have reported that the N protein of paramyxoviruses constitutes vRNP in concert with the P and L proteins and viral genomic RNA (David M.Knipe and M.Howley, 2020), we used MuV-N to represent the location of MuV (Figure 1A, red panel).

Further evaluation of the LC3-I to LC3-II conversion using immunoblotting confirmed the autophagy activation. Notably, despite having a molecular weight of 16 kDa more than LC3-I (14 kDa), LC3-II migrates on SDS-PAGE more quickly than LC3-I because of its extreme hydrophobicity. Our results showed that cells infected with MuV contained more LC3-II than mock-infected cells, consistent with the confocal microscope detection (Figure 2A). Since the ratio of LC3-II to LC3-I is thought to be a reliable indicator of autophagic activity (Klionsky, 2016), the quantification of this ratio is also evaluated. As shown in Figure 2B, the ratio of LC3-II to LC3-I was significantly higher in virus-infected groups than those in control group. Concurrently, MuV titers increased in a time-dependent manner from 1 to 4 days post-infection (dpi) (Figure 2C). These findings collectively confirm MuV-triggered autophagy in Vero cells.

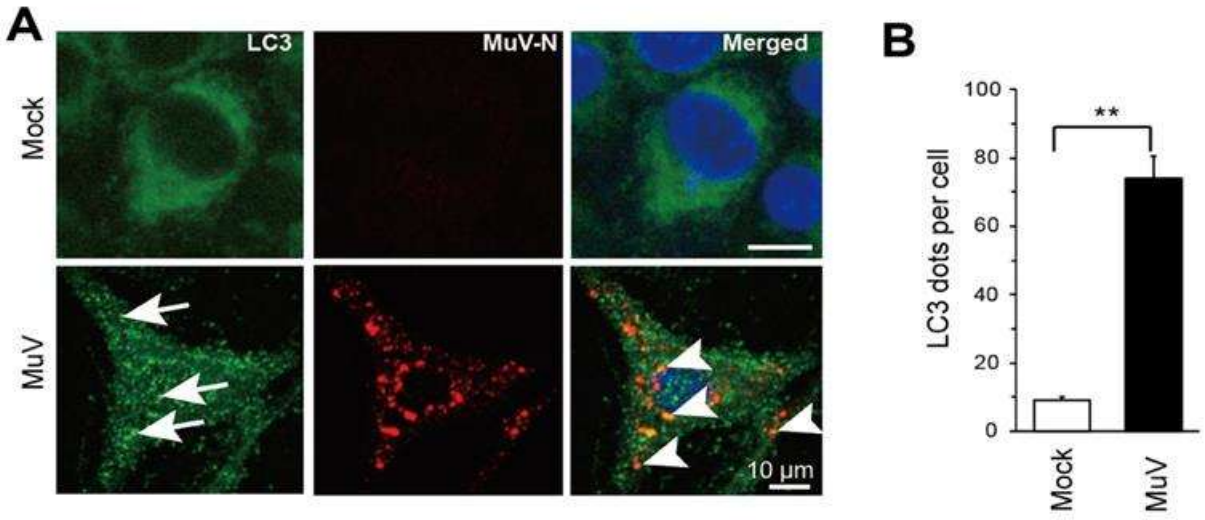

Figure 1: MuV induces LC3 lipidation in Vero cells

(A) Vero cells were mock-infected or infected with SP-A strain MuV and stained with anti-LC3. The viral N protein was used as an indication of viral infection. The autophagy marker LC3 (green) aggregates as granules and colocalizes with MuV-N (red) protein (white arrows). Scale bar: 10 μm. (B) Quantification of LC3 puncta/cell in Vero cells was performed from randomly selected cells. Values are expressed as the mean ± SD. **, $p < 0.01$.

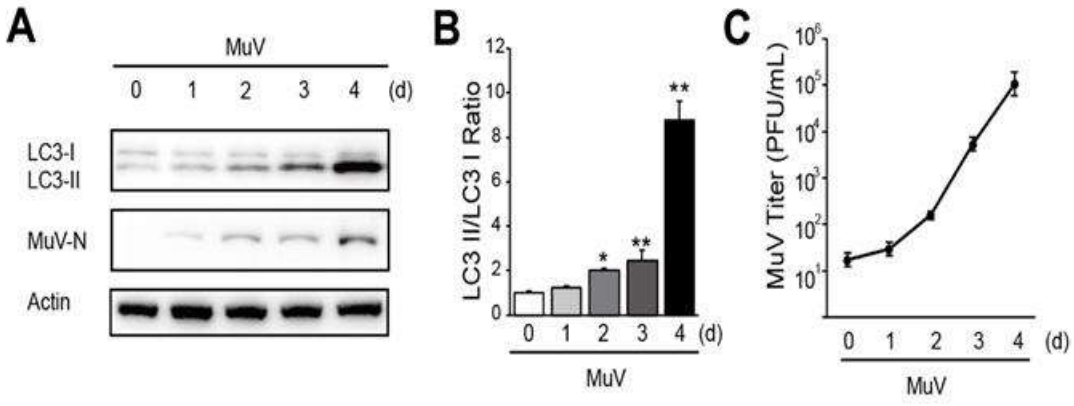

Figure 2: MuV infection causes upregulation of LC3-II/LC3-I ratio in Vero cells

(A) Cells were infected with MuV at an MOI of 0.1, and cell lysates were collected at 1, 2, 3, and 4 days. Cell lysates were subjected to autophagy analysis by western blot. Actin was used as a loading control. (B) LC3 expression was quantitated by densitometric analysis and normalized to mock infection, which was arbitrarily set to a value of 1.0. The LC3-II/LC3-I ratio, which is a hallmark of autophagy, increases with the progression of MuV infection. (C) Growth kinetic of MuV in Vero cells.

MuV induces autophagic structure accumulation in Vero cells

Upon autophagy initiation, an isolation membrane, also known as a phagophore, engulfs a portion of the cytoplasm to form the characteristic double-membraned autophagosome. This organelle subsequently fuses with a lysosome, resulting in an autolysosome where lysosomal enzymes degrade its contents (Klionsky, 2016). To enhance the visualization of autophagic compartments in MuV-infected Vero cells, we employed transmission electron microscopy (TEM) for ultrastructural analysis. Compared to fluorescence microscopy, the resolution of TEM is superior and is recognized as the golden standard for autophagy detection. Results showed that autophagic structures were infrequent in the uninfected cells (Figure 3A). However, there were different types of double-membrane structures in the cytosol of infected cells. Strongly flattened vesicles with partially or fully closed membranes that exhibited an inclination to absorb cytoplasmic material were identified as phagophores (Figure 3B and 3F). Notably, some double-membrane vesicles (diameter: 500 to 1000 nm) that resembled autophagosomes were frequently visually empty or contained one or more virus particles (Figures 3E, 3F, and 3H). Strikingly, large single-membrane autolysosomes (2-8 μm) occupied substantial cytoplasmic space, in some infected Vero cells (Figure 3G). These larger autolysosomes could arise from fusion events. Interestingly, autophagosomes and autolysosomes contained an array of membrane vesicles of varied sizes, including those within the MuV size range (50-600 nm) (Figure 3, arrowheads). These direct observation of autophagic structure accumulation indicates a continuous formation and accumulation of autophagosomes in MuV-infected Vero cells.

Based on the results of Figures 2A and 2B, upregulation of autophagy in MuV-infected Vero cells persists for days, rather than hours. Moreover, MuV titers increase at the same timeline (Figure 2C). Combined with the co-localization of LC3 puncta and MuV-N (Figure 1A, arrowheads), we inferred that autophagic structures are accompanied by the replication of MuV in Vero cells. Thus, we co-stained the MuV with the lysosomal marker LAMP1. Immunostaining results showed that LAMP1 co-localized with MuV-N in virus-infected cells (Figure 3I), suggesting capsids of MuV were inside lysosomes or autolysosomes. Given the presence of viral particles in autophagic structures (Figure 1A and Figure 4, arrowheads), these findings substantiate MuV's association with autophagosomes and autolysosomes.

According to the lifecycle of MuV, viruses are completely assembled by the budding of the cluster of vRNP complexes, synthesized in the cytoplasm, and budded from the cell surface. Additionally, the glycoproteins of paramyxoviruses are thought to be delivered to the plasma membrane by the exocytic pathway (Chang and Dutch, 2012). Functionally, lysosomes can also release viral contents in the form of lysosomal exocytosis into extracellular space (Chen et al. 2021). Therefore, we evaluated the budding process of MuV through TEM. Morphological changes related to the release of mumps virus in inoculated cultures were observed near the cell surface in our study. The surface-adjacent structures have a uniform width of approximately 500-1000 nm, containing black-dotted viruses or circled viruses (Figures 5A and 5B, arrows).

Consistent with the results of Figure 3, there were phagophores, lysosomes, and autolysosomes near the virus-budding surface (Figures 5A and 5B). As expected, the presence of viruses within lysosomes was also observed through ultrastructural analysis (Figures 6A and 6B, arrows). Collectively, these observations affirm that MuV replication coincides with the autophagic process

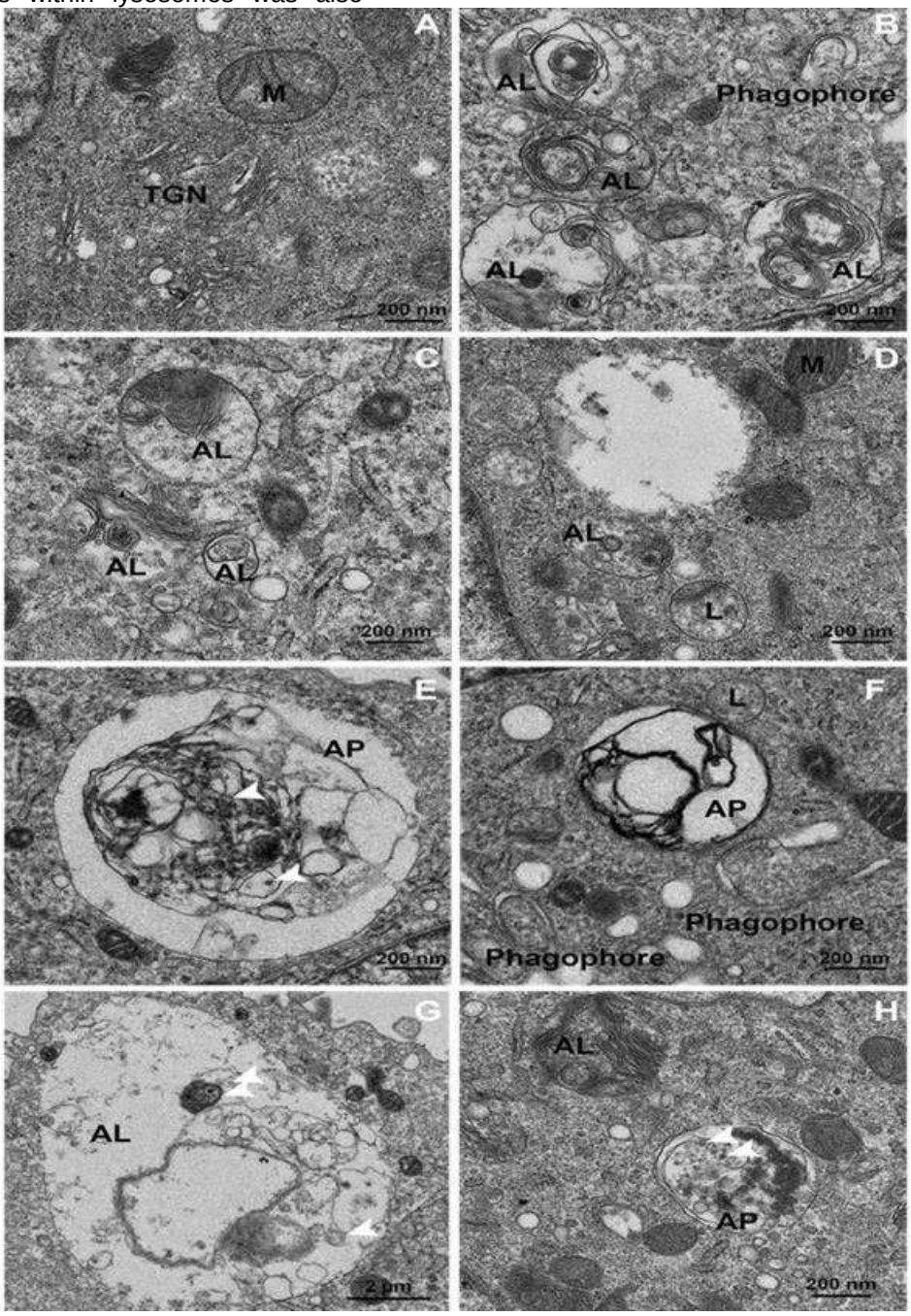

Figure 3: MuV induces the accumulation of autophagic structures in Vero cells

Cells were collected, prepared into ultrathin sections, and imaged under transmission electron microscopy. TEM showed the internal ultrastructure of the control group (A) and the infected group (B-H). In MuV-infected Vero cells, cup-shaped phagophores, double-membraned autophagosomes (AP), and single-membraned autolysosomes (AL) were observed. The location of MuV was indicated by white arrows. M, mitochondrion; L, lysosome; TGN, trans-Golgi network; AL, autolysosome; AP, autophagosome. Bars are as indicated. (G) Representative electron micrograph of MuV vesicles in a large autolysosome (AL).

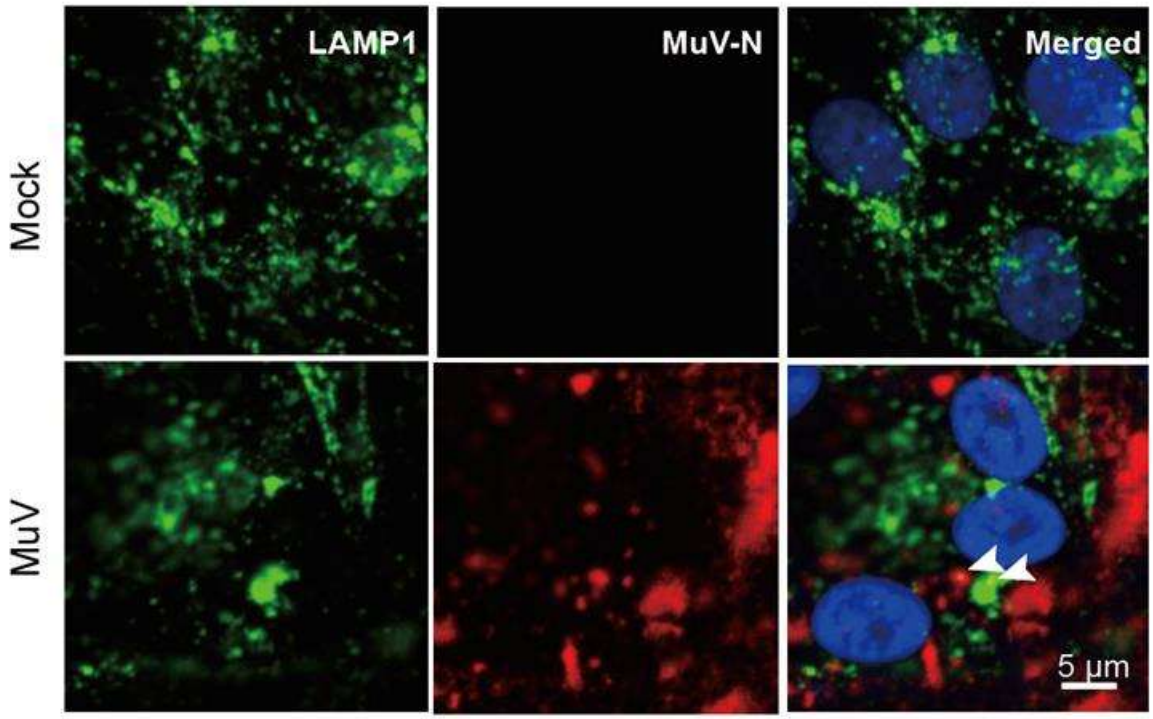

Figure 4: MuV-N colocalize with LAMP1 in Vero cells

Vero cells were mock-infected or infected with genotype F MuV and stained with anti-LAMP1. The lysosomal membrane protein LAMP1 (green) colocalized with MuV-N (red) protein (white arrows). Scale bar: 5 μm.

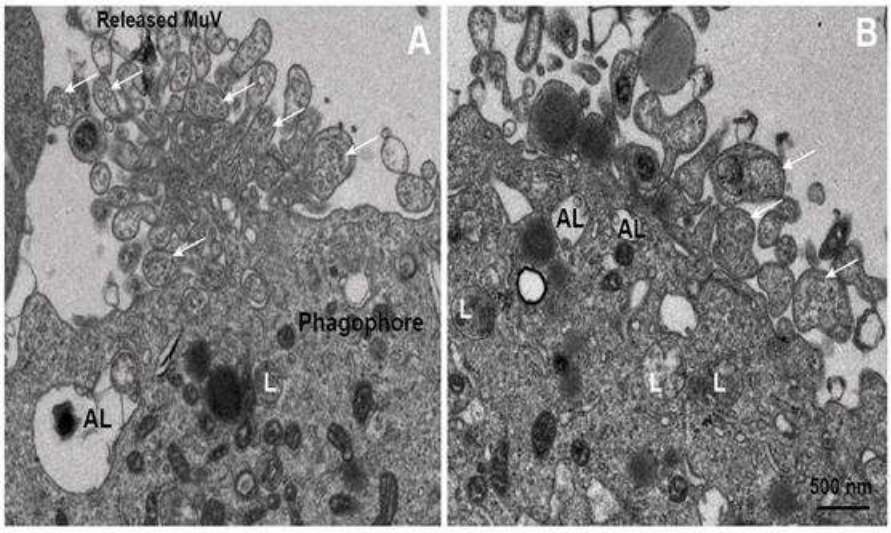

Figure 5: In MuV-infected Vero cells, some phagophores, lysosomes (L), and autolysosomes (AL) were observed near the surface of released MuV. The released MuV was indicated by white arrows. Scale bar: 500 nm.

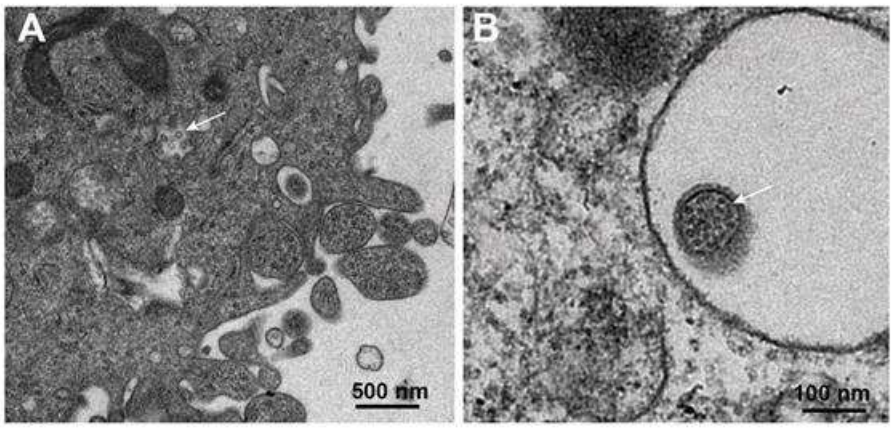

Figure 6: MuV was observed inside lysosomes in infected Vero cells. Arrows indicate viruses. Bars are as indicated.

DISCUSSION

Autophagy, a conserved lysosomal degradation pathway, plays a pivotal role in capturing and combatting invading viruses within the host (Choi et al. 2018). However, viruses have evolved strategies to co-opt host autophagy and related membrane vesicular transport systems to facilitate their replication (Levine et al. 2011). Studies have shown that autophagy can inhibit infection by eliminating herpes simplex virus (HSV-1) and Sindbis virus (SINV), among others (Orvedahl et al. 2007, 2010; Choi et al. 2018). At the same time, viruses that successfully parasitize the human body have evolved corresponding mechanisms to use autophagy to promote their own replication. For example, influenza A virus (IAV) hijacks autophagy through matrix protein M2 and accessory protein PB1-F2 to promote the production of infectious virions (Wang et al. 2019b, 2019a, 2021). Human parainfluenza virus type 3 (HPIV3) matrix protein M induces mitophagy by interacting with LC3 to weaken the immune response and promote infection (Ding et al. 2017). Moreover, the severe acute respiratory syndrome coronavirus 2 (SARS-CoV-2) accessory protein ORF3a inhibits its degradation by autophagy by inhibiting the fusion of autophagosomes and lysosomes (Miao et al. 2021). Among the *Paramyxoviridae* family, which encompasses measles virus (MeV), Newcastle disease virus (NDV), respiratory syncytial virus (RSV), and parainfluenza viruses, disparate autophagy responses have been documented. For instance, sustained autophagy enhances MeV infectivity (Richetta et al. 2013), while NDV exploits autophagy for virus production (Meng et al. 2012). RSV induces autophagy in various cell types including lung epithelial cells, macrophages, and dendritic cells (Chiok et al. 2022). Similarly, Sendai virus (SeV) requires autophagy for replication in L929 cells (Subramanian et al. 2018). Additionally, HPIV3 thwarts autophagosome-lysosome fusion, causing incomplete autophagy that enhances virus production (Ding et al. 2014). Notably, Nipah virus (NiV), Hendra virus (HeV), and MuV glycoprotein F were found to induce autophagy in Vero cells, suggesting a commonality among paramyxoviruses (Delpeut et al. 2012). Our study adds to this by demonstrating that attenuated MuV induces autophagy in Vero cells, supported by LC3 lipidation, elevated LC3-II/LC3-I ratio, and direct electron microscopic observations of autophagic processes (Figure 1 to Figure 3).

It is known that many viruses replicate in specific intracellular compartments called virus factories. These are supposed to increase the efficiency of viral replication by acting as a physical scaffold to concentrate viral components. The cytoskeleton and cellular membranes are frequently rearranged as a result of the creation of virus replication sites (Netherton et al. 2007). Autophagy involves dynamic membrane rearrangements, resulting in the formation of double-membraned autophagosomes (diameters 500 to 1000 nm) through phagophore or isolation membrane enclosure of cytoplasmic components. The subsequent fusion of autophagosomes with lysosomes forms autolysosomes where contents are degraded (Mizushima and Komatsu, 2011; Deretic, 2021). RNA viruses, including poliovirus and hepatitis C virus, utilize autophagic membranes to assemble replication complexes in the cytoplasm (Wileman, 2006). In MuV-inoculated Vero cells, transmission electron microscopy revealed crescent-shaped phagophores, double-membraned autophagosomes (500-1000 nm), and single-membraned autolysosomes (Figures 3B-2H). Interestingly, some vesicles exhibited large luminal volumes (2-8 μm) (Figure 3G), and electron-dense MuV particles (55-600 nm diameter) were observed in the lumen (Figures 3E and 3G). The co-localization of LC3 and LAMP1 with MuV supports autophagy during MuV replication (Figure 4). Moreover, upregulation of autophagy in MuV-infected Vero cells persists for days, rather than hours (Figure 2A and 2B). In consistency with the MuV titer increase at the same timeline (Figure 2C),

MuV might induce autophagy to construct scaffolds for vRNP complexes or to hijack the autophagic structures to egress. Alternatively, the virus precursor that entered autophagic structures could be degraded inside them. Assessing the pro-survival or anti-survival impact of MuV-induced autophagy on cells will contribute to understanding the underlying mechanism. Finally, observation of MuV in lysosomes and lysosomes near the budding surface of MuV (Figures 5 and 6) indicates lysosomal exocytosis may play an important role in the production of MuV.

Vero cells, a continuous cell line established from the cells of the African green monkey kidney in 1962, are highly permissive to the growth of varieties of viruses. Since most normal cells produce interferons to fight against viruses, while Vero cells are interferon deficient. This cell line is also preferred for in vitro culture of severe acute respiratory syndrome coronavirus (SARS-CoV). The SARS coronavirus was isolated using Vero E6 cells during 2003 SARS-CoV (Papazian et al. 2003) and 2019 SARS-CoV-2 outbreak. Autophagy induced in SARS-CoV-2 infected Vero cells was reported to support its production (Hui et al. 2021). The relative susceptibility of available continuous cell lines for virus growth is yet not fully investigated. Here, we propose that host autophagy in Vero cells may be a key factor because MuV did not induce prominent autophagic structures in other cell lines including A549 and Hela cells (data not shown). To better understand the mechanism, evaluation of MuV-induced autophagy on various cell lines will be helpful.

Based on the sequence of *SH* and *HN* genes, MuV exists in 12 distinct genotypes, serving as focal points for surveillance as designated by the WHO. Currently, vaccine strains used globally are of genotypes A, B, H, or N (Latner and Hickman, 2015). Despite the belief that MuV is serologically monotypic, some investigations have revealed the production of MuV genotype-specific antibodies (Kubota et al. 2016). Consequently, the antigenic diversity among various genotype types raises questions regarding MuV immunization and spontaneous infection. The MuV strain employed in our study belongs to genotype F (Liang et al. 2019). Notably, genotype F MuV has sustained circulation within China over the last two decades, and it is also prevalent across ten additional countries spanning North America, Europe, and Asia (Cui et al. 2017; Su et al. 2022). Consequently, enhancing our comprehension of genotype F assumes pivotal importance for global public health considerations.

CONCLUSIONS

In conclusion, our findings offer compelling evidence of autophagy's involvement in the replication of the genotype F strain. We have also demonstrated that the lysosomes and autolysosomes are important cellular factors in the process of MuV production. Delving deeper into the examination of autophagy induced by other MuV strains will provide valuable insights into the shared mechanisms underpinning MuV replication. Furthermore, the identification of viral factors and mechanisms that drive MuV-induced autophagy holds the potential to significantly enrich our comprehension of virus-host interactions, ultimately illuminating their pivotal roles in the context of pathogenesis.

Supplementary materials

The supplementary material / supporting for this article can be found online and downloaded at: https://www.isisn.org/article/

Author contributions

Conceptualization, methodology, investigation, data curation, manuscript preparation, and funding acquisition, H. W.

Funding statement

This study was supported by the Guangdong Basic and Applied Basic Research Foundation (2021A1515010509).

Institutional Review Board Statement

The study was approved by the Bioethical Committee of the …….

Informed Consent Statement

Not applicable.

Data Availability Statement

All of the data is included in the article/Supplementary Material.

Acknowledgments

This work was supported by the Guangdong Basic and Applied Basic Research Foundation (2021A1515010509).

Conflict of interest

The authors declare no conflict of interest.

Peer Review: ISISnet follows double blind peer review policy and thanks the anonymous reviewer(s) for their contribution to the peer review of this article.

REFERENCES

Ammayappan, A., Russell, S. J., and Federspiel, M. J. (2016). Recombinant mumps virus as a cancer therapeutic agent. *Mol. Ther. - Oncolytics* 3, 16019. doi:10.1038/mto.2016.19.

Briggs, K., Wang, L., Nagashima, K., Zengel, J., Tripp, R. A., and He, B. (2020). Regulation of Mumps Virus Replication and Transcription by Kinase RPS6KB1. *J. Virol.* 94. doi:10.1128/jvi.00387-20.

Chang, A., and Dutch, R. E. (2012). Paramyxovirus fusion and entry: Multiple Paths to a common end. *Viruses* 4, 613–636. doi:10.3390/v4040613.

Chen, D., Zheng, Q., Sun, L., Ji, M., Li, Y., Deng, H., et al. (2021). ORF3a of SARS-CoV-2 promotes lysosomal exocytosis-mediated viral egress. *Dev. Cell* 56, 3250-3263.e5. doi:10.1016/j.devcel.2021.10.006.

Chiok, K., Pokharel, S. M., Mohanty, I., Miller, L. G., Gao, S.-J., Haas, A. L., et al. (2022). Human Respiratory Syncytial Virus NS2 Protein Induces Autophagy by Modulating Beclin1 Protein Stabilization and ISGylation. *MBio* 13, 1–15.

Choi, Y., Bowman, J. W., and Jung, J. U. (2018). Autophagy during viral infection - A double-edged sword. *Nat. Rev. Microbiol.* 16, 341–354. doi:10.1038/s41579-018-0003-6.

Connell, A. R., Connell, J., Leahy, T. R., and Hassan, J. (2020). Mumps Outbreaks in Vaccinated Populations—Is It Time to Re-assess the Clinical Efficacy of Vaccines? *Front. Immunol.* 11. doi:10.3389/fimmu.2020.02089.

Cui, A., Rivailler, P., Zhu, Z., Deng, X., Hu, Y., Wang, Y., et al. (2017). Evolutionary analysis of mumps viruses of genotype F collected in mainland China in 2001-2015. *Sci. Rep.* 7, 1–7. doi:10.1038/s41598-017-17474-z.

David M.Knipe, and M.Howley, P. (2020). *Fields virology*. Available at: www.journal.uta45jakarta.ac.id.

Delpeut, S., Rudd, P. A., Labonté, P., and von Messling, V. (2012). Membrane Fusion-Mediated Autophagy Induction Enhances Morbillivirus Cell-to-Cell Spread. *J. Virol.* 86, 8527–8535. doi:10.1128/jvi.00807-12.

Deretic, V. (2021). Autophagy in inflammation, infection, and immunometabolism. *Immunity* 54, 437–453. doi:10.1016/j.immuni.2021.01.018.

Ding, B., Zhang, G., Yang, X., Zhang, S., Chen, L., Yan, Q., (2014). Phosphoprotein of human parainfluenza virus type 3 blocks autophagosome-lysosome fusion to increase virus production. *Cell Host Microbe* 15, 564–577. doi:10.1016/j.chom.2014.04.004.

Ding, B., Zhang, L., Li, Z., Zhong, Y., Tang, Q., Qin, Y., et al. (2017). The Matrix Protein of Human Parainfluenza Virus Type 3 Induces Mitophagy that Suppresses Interferon Responses. *Cell Host Microbe* 21, 538-547.e4. doi:10.1016/j.chom.2017.03.004.

Forgione, R. E., Di Carluccio, C., Kubota, M., Manabe, Y., Fukase, K., Molinaro, A., et al. (2020). Structural basis for Glycan-receptor binding by mumps virus hemagglutinin-neuraminidase. *Sci. Rep.* 10, 1–13. doi:10.1038/s41598-020-58559-6.

Gokhale, D. V., Brett, T. S., He, B., King, A. A., and Rohani, P. (2023). Disentangling the causes of mumps reemergence in the United States. *Proc. Natl. Acad. Sci. U. S. A.* 120, 1–10. doi:10.1073/pnas.2207595120.

Guichard, A., Nizet, V., and Bier, E. (2014). RAB11 - mediated trafficking in host – pathogen interactions. *Nat. Publ. Gr.* 12, 624–634. doi:10.1038/nrmicro3325.

Hui, X., Zhang, L., Cao, L., Huang, K., Zhao, Y., Zhang, Y., et al. (2021). SARS-CoV-2 promote autophagy to suppress type I interferon response. *Signal Transduct. Target. Ther.* 6, 2020–2022. doi:10.1038/s41392-021-00574-8.

Katoh, H., Nakatsu, Y., Kubota, T., Sakata, M., Takeda, M., and Kidokoro, M. (2015). Mumps Virus Is Released from the Apical Surface of Polarized Epithelial Cells, and the Release Is Facilitated by a Rab11-Mediated Transport System. *J. Virol.* 89, 12026–12034. doi:10.1128/jvi.02048-15.

Klionsky, D. J. et al. (2016). Guidelines for the use and interpretation of assays for monitoring autophagy (3rd edition). *Autophagy* 12, 1–222. doi:10.1080/15548627.2015.1100356.

Kubota, M., Matsuoka, R., Suzuki, T., and Yonekura, K. (2019). Molecular Mechanism of the Flexible Glycan Receptor Recognition by Mumps Virus. *J. Virol.* 93, 1–13.

Kubota, M., Takeuchi, K., Watanabe, S., Ohno, S., Matsuoka, R., Kohda, D., et al. (2016). Trisaccharide containing α2,3-linked sialic acid is a receptor for mumps virus. *Proc. Natl. Acad. Sci. U. S. A.* 113, 11579–11584. doi:10.1073/pnas.1608383113.

Latner, D. R., and Hickman, C. J. (2015). Remembering Mumps. *PLoS Pathog.* 11, 16–19. doi:10.1371/journal.ppat.1004791.

Levine, B., Mizushima, N., and Virgin, H. W. (2011). Autophagy in immunity and inflammation. *Nature* 469, 323–335. doi:10.1038/nature09782.

Liang, Y., Che, Y., Yang, B., Zhan, F., Li, H., Guan, X., (2019). Immunogenicity and safety of an F-Genotype attenuated mumps vaccine in healthy 8- to 24-month-old children. *J. Infect. Dis.* 219, 50–58.

doi:10.1093/infdis/jiy469.

Meng, C., Zhou, Z., Jiang, K., Yu, S., Jia, L., Wu, Y., (2012). Newcastle disease virus triggers autophagy in U251 glioma cells to enhance virus replication. *Arch. Virol.* 157, 1011–1018. doi:10.1007/s00705-012-1270-6.

Miao, G., Zhao, H., Li, Y., Ji, M., Chen, Y., Shi, Y., (2021). ORF3a of the COVID-19 virus SARS-CoV-2 blocks HOPS complex-mediated assembly of the SNARE complex required for autolysosome formation. *Dev. Cell* 56, 427-442.e5. doi:10.1016/j.devcel.2020.12.010.

Mizushima, N., and Komatsu, M. (2011). Autophagy: Renovation of cells and tissues. *Cell* 147, 728–41. doi:10.1016/j.cell.2011.10.026.

Netherton, C., Moffat, K., Brooks, E., and Wileman, T. (2007). A Guide to Viral Inclusions, Membrane Rearrangements, Factories, and Viroplasm Produced During Virus Replication. *Adv. Virus Res.* 70, 101–182. doi:10.1016/S0065-3527(07)70004-0.

Noboru Mizushima and Beth Levine (2010). autophagy in mammalian differentiation. *Nat Cell Biol* 12, 823–830. doi:10.1038/jid.2014.371.

Orvedahl, A., Alexander, D., Tallóczy, Z., Sun, Q., Wei, Y., Zhang, W., (2007). HSV-1 ICP34.5 Confers Neurovirulence by Targeting the Beclin 1 Autophagy Protein. *Cell Host Microbe* 1, 23–35. doi:10.1016/j.chom.2006.12.001.

Orvedahl, A., Macpherson, S., Jr, R. S., Tallóczy, Z., Zou, Z., and Levine, B. (2010). Autophagy Protects against Sindbis Virus Infection of the Central Nervous System. *Cell Host Microbe* 7, 115–127. doi:10.1016/j.chom.2010.01.007.

Papazian, L., Forel, J.-M., Gacouin, A., Penot-Ragon, C., Perrin, G., Loundou, A., (2003). A Novel Coronavirus Associated with Severe Acute Respiratory Syndrome Thomas. *N. Engl. J. Med.* 348, 1953–1965.

Richetta, C., Grégoire, I. P., Verlhac, P., Azocar, O., Baguet, J., Flacher, M., (2013). Sustained Autophagy Contributes to Measles Virus Infectivity. *PLoS Pathog.* 9. doi:10.1371/journal.ppat.1003599.

Rubin, S. A., Link, M. A., Sauder, C. J., Zhang, C., Ngo, L., Rima, B. K., et al. (2012). Recent Mumps Outbreaks in Vaccinated Populations: No Evidence of Immune Escape. *J. Virol.* 86, 615–620. doi:10.1128/jvi.06125-11.

Shan, H., Su, X., Li, T., Qin, Y., Zhang, N., Yang, L., (2021). Structural plasticity of mumps virus nucleocapsids with cryo-EM structures. *Commun. Biol.* 4, 1–11. doi:10.1038/s42003-021-02362-0.

Su, S. Bin, Chang, H. L., and Chen, K. T. (2020). Current status of mumps virus infection: Epidemiology, pathogenesis, and vaccine. *Int. J. Environ. Res. Public Health* 17. doi:10.3390/ijerph17051686.

Su, Y., Liu, J., Liu, M., Li, M., Gao, F., Li, C., (2022). Genotype F Mumps Viruses Continue to Circulate in China, From 1995 to 2019. *Front. Virol.* 2, 1–8. doi:10.3389/fviro.2022.901618.

Subramanian, G., Kuzmanovic, T., Zhang, Y., Peter, C. B., Veleeparambil, M., Chakravarti, R., et al. (2018). A new mechanism of interferon's antiviral action: Induction of autophagy, essential for paramyxovirus replication, is inhibited by the interferon stimulated gene, TDRD7. *PLoS Pathog.* 14, 1–25. doi:10.1371/journal.ppat.1006877.

Ueo, A., Kubota, M., Shirogane, Y., and Ohno, S. (2020). Lysosome-Associated Membrane Proteins Support the Furin-Mediated Processing of the Mumps Virus Fusion Protein. *J. Virol.* 94, 1–12.

Wang, R., Zhu, Y., Lin, X., Ren, C., Zhao, J., Wang, F., et al. (2019a). Influenza M2 protein regulates MAVS-mediated signaling pathway through interacting with MAVS and increasing ROS production. *Autophagy* 15, 1163–1181. doi:10.1080/15548627.2019.1580089.

Wang, R., Zhu, Y., Ren, C., Yang, S., Tian, S., Chen, H., (2021). Influenza A virus protein PB1-F2 impairs innate immunity by inducing mitophagy. *Autophagy* 17, 496–511. doi:10.1080/15548627.2020.1725375.

Wang, R., Zhu, Y., Zhao, J., Ren, C., Li, P., Chen, H., (2019b). Autophagy Promotes Replication of Influenza A Virus In Vitro. *J. Virol.* 93, 1–17. doi:10.1128/jvi.01984-18.

Wileman, T. (2006). Sites for Virus Replication. *Science*, 875–878.

Wu, H., Zhao, X., Wang, F., Jiang, Q., Shi, L., Gong, M., (2017). Mouse testicular cell type-specific antiviral response against mumps virus replication. *Front. Immunol.* 8. doi:10.3389/fimmu.2017.00117.

Yoshii, S. R., and Mizushima, N. (2017). Monitoring and measuring autophagy. *Int. J. Mol. Sci.* 18, 1–13. doi:10.3390/ijms18091865.

Zhang, X., Sridharan, S., Zagoriy, I., Eugster Oegema, C., Ching, C., Pflaesterer, T., (2023). Molecular mechanisms of stress-induced reactivation in mumps virus condensates. *Cell* 186, 1877–1894. doi:10.1016/j.bpj.2021.11.1982.